

Gravitational Wave Emission from a Primordial Black Hole Inspiring inside a Compact Star: a Novel Probe for Dense Matter Equation of State

ZE-CHENG ZOU (邹泽城) ¹ AND YONG-FENG HUANG (黄永锋) ^{1,2}

¹*School of Astronomy and Space Science, Nanjing University, Nanjing 210023, China*

²*Key Laboratory of Modern Astronomy and Astrophysics (Nanjing University), Ministry of Education, Nanjing 210023, China*

ABSTRACT

Primordial black holes of planetary masses captured by compact stars are widely studied to constrain their composition fraction of dark matter. Such a capture may lead to an inspiral process and be detected through gravitational wave signals. In this Letter, we study the post-capture inspiral process by considering two different kinds of compact stars, i.e., strange stars and neutron stars. The dynamical equations are numerically solved and the gravitational wave emission is calculated. It is found that the next generation gravitational wave detectors can detect the inspiring of a $10^{-5} M_{\odot}$ primordial black hole at a distance of 1 kpc. A Jovian-mass case can even be detected at megaparsecs. Moreover, the kilohertz gravitational wave signal shows significant differences for strange stars and neutron stars, potentially making it a novel probe to the dense matter equation of state.

Keywords: Gravitational waves (678); Neutron stars (1108); Nuclear astrophysics (1129); Primordial black holes (1292)

1. INTRODUCTION

Primordial black holes (PBHs; Zel'dovich & Novikov 1967) can be formed through a vast range of mechanisms. For example, they may be generated due to the density inhomogeneity in the early universe (for a review, see Khlopov 2010). Although having not been directly detected yet, PBHs are considered to be a candidate for dark matter (for a review, see Carr & Kühnel 2020). To constrain PBHs' composition fraction of dark matter, the event rate of collisions between planetary-mass PBHs and compact stars has been widely discussed and the corresponding electromagnetic emissions have been extensively studied (e.g., Capela et al. 2013; Pani & Loeb 2014; Abramowicz et al. 2018; Génolini et al. 2020). Interestingly, during such a collision, the PBH-compact star system will also emit gravitational waves (GWs) as the PBH accretes matter from the compact star. Kurita & Nakano (2016) and East & Lehner (2019) studied the GW signals from an accreting PBH, which is assumed to have plunged into its compact companion and stays at the exact center of the neutron star (NS). Horowitz & Reddy (2019) and Génolini et al. (2020) studied the GW emission during the inspiring process of a PBH inside a NS, but their treatment of the dynamics and the compact star structure is still preliminary.

On the other hand, the equation of state (EoS) of dense matter determines the structure of compact stars. According to the strange-quark matter hypothesis (Itoh 1970; Bodmer 1971; Farhi & Jaffe 1984; Witten 1984), pulsars may actually be strange stars (SSs) consisting of strange-quark matter (Alcock et al. 1986). The strange-quark matter is self-bound, thus strange dwarfs and even strange planets can stably exist. However, a $1.4 M_{\odot}$ SS has a radius very similar to that of a normal NS with comparable mass, thus it is hard to distinguish between these two types of compact stars via observations (Geng et al. 2015, 2021). An interesting method to identify strange quark objects is to search for very close-in binary systems containing a strange planet and a compact star (Geng et al. 2015; Kuerban et al. 2019, 2020; Wang et al. 2021). When the orbital radius of a planet is less than $\sim 5.6 \times 10^{10}$ cm or the orbital period is less than ~ 6100 s, then it cannot be a normal matter planet, but should be a strange planet, because the tidal force is too strong to allow any kinds of normal matter planets to stably exist there (Huang & Yu 2017; Kuerban et al. 2019, 2020). However, in these close-in “planetary” systems, there is still a possibility that the planetary-mass object is actually a PBH. We thus need to further scrutinize its nature.

GW astronomy may shed new light on the study of compact star structure. Tidal deformability and maximal mass of compact stars, which can be hinted through GW signals from double compact star mergers (for a review, see Guerra Chaves & Hinderer 2019), may reflect the internal composition and structure of compact stars (e.g., Wang et al. 2021). In fact, the observations of GW170817 have already put useful constraints on the tidal deformability of “neutron stars” (Annala et al. 2018; Abbott et al. 2018, 2019). However, these constraints are still too weak to pin down the EoS (Lai et al. 2019; Shibata et al. 2019; Mondal & Gulminelli 2021). In this Letter, we will study the GW emission produced by a PBH inspiraling inside a compact star. Different from a strange planet, a PBH can inspiral and tunnel inside the compact star, producing special GW signals. Two kinds of EoSs will be assumed for the compact stars in our calculations, i.e., a strange-quark matter EoS and a hadronic matter EoS. The results will help us judge whether the close-in planetary-mass object is a strange planet or a PBH.

The structure of this Letter is as follows. In Section 2, we describe the model by setting up the equations of motion and compact star structure. Numerical results on the dynamics are then presented in Section 3. In Section 4, the GW emissions are calculated and analyzed. Finally, we summarize and discuss our results in Section 5. Throughout this Letter, a natural unit system of $c = G = \hbar = 1$ is adopted.

2. MODEL SETUP

As a PBH inspirals inside a compact star, it gradually loses its orbital kinetic energy through interactions with compact star matter. We focus on three main channels — dynamical friction, accretion, and GW emission (Génolini et al. 2020). Moreover, we assume that the trajectory of the PBH within the compact star is quasi-circular and do not consider any effects of ellipticity. This condition can be guaranteed by the tidal dissipation and various circularization effects (Ogilvie 2014).

2.1. Dynamical Friction

A wake is produced when the PBH (of mass m_{PBH}) moves through surrounding medium (with a density of ρ and the sound speed c_s). The wake will then exert a gravitational drag force on the PBH, known as the dynamical friction force (Ostriker 1999). For a circular orbit, the force can be written on the basis of the radial (\hat{r}) and azimuthal ($\hat{\varphi}$) components as (Kim & Kim 2007)

$$\mathbf{F}_{\text{DF}} = -\frac{4\pi\rho m_{\text{PBH}}^2}{v^2} (\mathcal{I}_r \hat{r} + \mathcal{I}_{\varphi} \hat{\varphi}), \quad (1)$$

where v is the relative speed of the PBH with respect to the medium. The coefficients \mathcal{I}_r and \mathcal{I}_φ are functions of the Mach number ($\mathcal{M} = v/c_s$) and the distance (r) between the PBH and the center of the compact star (Kim & Kim 2007):

$$\mathcal{I}_r = \begin{cases} \mathcal{M}^2 10^{3.51\mathcal{M}-4.22}, & \mathcal{M} < 1.1; \\ 0.5 \ln [9.33\mathcal{M}^2 (\mathcal{M}^2 - 0.95)], & 1.1 \leq \mathcal{M} < 4.4; \\ 0.3\mathcal{M}^2, & 4.4 \leq \mathcal{M}; \end{cases} \quad (2)$$

and

$$\mathcal{I}_\varphi = \begin{cases} 0.7706 \ln \left(\frac{1+\mathcal{M}}{1.0004-0.9185\mathcal{M}} \right) - 1.4703\mathcal{M}, & \mathcal{M} < 1.0; \\ \ln [330 (r/r_m) (\mathcal{M} - 0.71)^{5.72} \mathcal{M}^{-9.58}], & 1.0 \leq \mathcal{M} < 4.4; \\ \ln \left(\frac{r/r_m}{0.11\mathcal{M}+1.65} \right), & 4.4 \leq \mathcal{M}; \end{cases} \quad (3)$$

where $r_m = \sqrt{em_{\text{PBH}}}/(2v^2)$ (Cantó et al. 2011). However, the above expression of \mathcal{I}_φ fails for $\mathcal{M} \rightarrow 0$ because it gives an unphysically positive azimuthal drag force. In fact, in this deep subsonic phase, the circular-orbit dynamical friction is expected to be similar to the case of a straight trajectory (Ostriker 1999), i.e., $\mathcal{I}_\varphi = \ln [(1 + \mathcal{M})/(1 - \mathcal{M})] / 2 - \mathcal{M} \rightarrow \mathcal{M}^3/3$. To account for this asymptotic behavior, we use the following polynomial expansion for $\mathcal{M} \ll 1$,

$$\mathcal{I}_\varphi = \mathcal{M}^3/3 - 0.80352\mathcal{M}^4 + 7.68585\mathcal{M}^5. \quad (4)$$

This expression reduces to the solution of Ostriker (1999) for $\mathcal{M} \rightarrow 0$. When \mathcal{M} increases, it smoothly transits to Equation 3 at $\mathcal{M} = 0.08588$. So when $\mathcal{M} < 0.08588$, Equation 4 is applied instead of Equation 3 in our calculations.

2.2. Accretion

As the PBH accretes matter from the compact star, it also accumulates a negative momentum, resulting in a drag force of (Edgar 2004; Génolini et al. 2020)

$$\mathbf{F}_{\text{acc}} = -\dot{m}_{\text{PBH}}\mathbf{v}. \quad (5)$$

For a PBH with a finite velocity, the accretion rate is (Bondi 1952; Shima et al. 1985; Edgar 2004)

$$\dot{m}_{\text{PBH}} = \frac{4\pi\lambda\rho m_{\text{PBH}}^2}{(c_s^2 + v^2)^{3/2}}, \quad (6)$$

where λ is the accretion eigenvalue depending on the EoS of the accreted matter. Equation 6 is applicable for $m_{\text{PBH}} \ll M_{\text{CS}}$ (Richards et al. 2021), where M_{CS} is the mass of the compact star.

2.3. Structure of Compact Stars

The dynamical friction and accretion explicitly depend on ρ and c_s . Therefore, we shall obtain the compact star structure before further studying the equations of motion of the PBH. The structure of a non-rotating compact star is available by solving the Tolman-Oppenheimer-Volkoff equation (Tolman 1939; Oppenheimer & Volkoff 1939)

$$\frac{dP}{dr} = -\frac{M_r}{r^2}\rho \left(1 + \frac{P}{\rho}\right) \left(1 + \frac{4\pi r^3 P}{M_r}\right) \left(1 - \frac{2M_r}{r}\right)^{-1}, \quad (7)$$

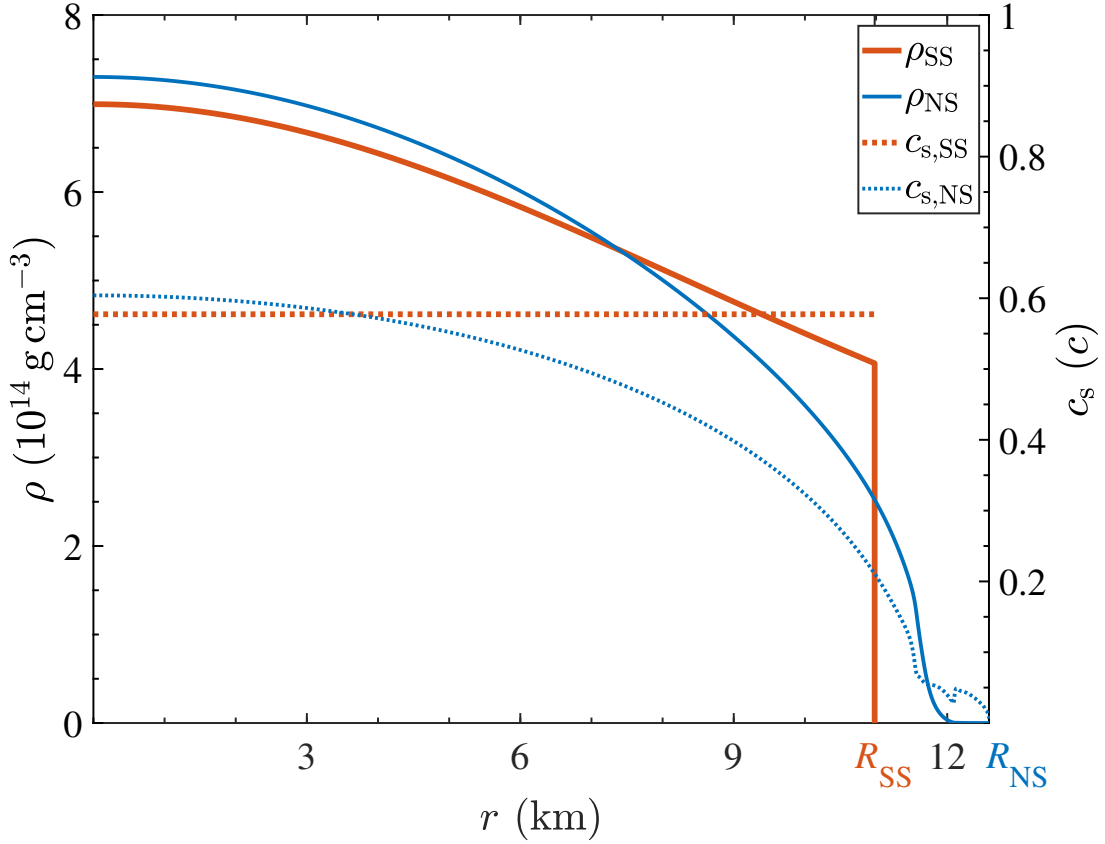


Figure 1. Density (solid curves; left y -axis) and sound speed (dotted curves; right y -axis) profiles of a $1.4 M_{\odot}$ strange star (SS, thick curves) and neutron star (NS, thin curves).

where P is the pressure, and M_r is the mass within the radius r so that $dM_r/dr = 4\pi r^2 \rho$. To solve Equation 7, one needs the EoS of compact star matter. Two typical kinds of compact stars, SSs and normal NSs, are considered in our study. For SSs, we adopt the simple bag model with massless quarks (Farhi & Jaffe 1984), whose EoS reads $P = (\rho - 4B)/3$. The bag constant B is taken as 57 MeV fm^{-3} . For NSs, we use the hadronic BSk 24 EoS¹ (Potekhin et al. 2013; Pearson et al. 2018). The sound speed is calculated from $c_s = \sqrt{dP/d\rho}$.

The density and sound speed profiles of a $1.4 M_{\odot}$ SS and NS are shown in Figure 1. The SS has a smaller radius ($R_{\text{SS}} = 11.0 \text{ km}$) than the NS ($R_{\text{NS}} = 12.6 \text{ km}$). Moreover, the SS has a rather uniform density and sound speed profile with a sharp edge, while the NS's density and sound speed vary significantly from its center to surface. These differences indicate that the drag force exerted on the inspiraling PBH may be different in these two cases.

For the parameter λ , although there are analytical expressions for EoSs when the adiabatic index is $\Gamma \geq 1$ (Richards et al. 2021; Aguayo-Ortiz et al. 2021), no simple expression is available when $\Gamma < 1$ (at the phase transition region of a NS; Potekhin et al. 2013) and $\Gamma \rightarrow \infty$ (at the surface of a SS; Xia et al. 2021). So, we use a commonly-used value of $\Gamma = 4/3$ in our calculations, which naturally gives $\lambda = 1/\sqrt{2}$ (Génolini

¹ <http://www.ioffe.ru/astro/NSG/BSk/>

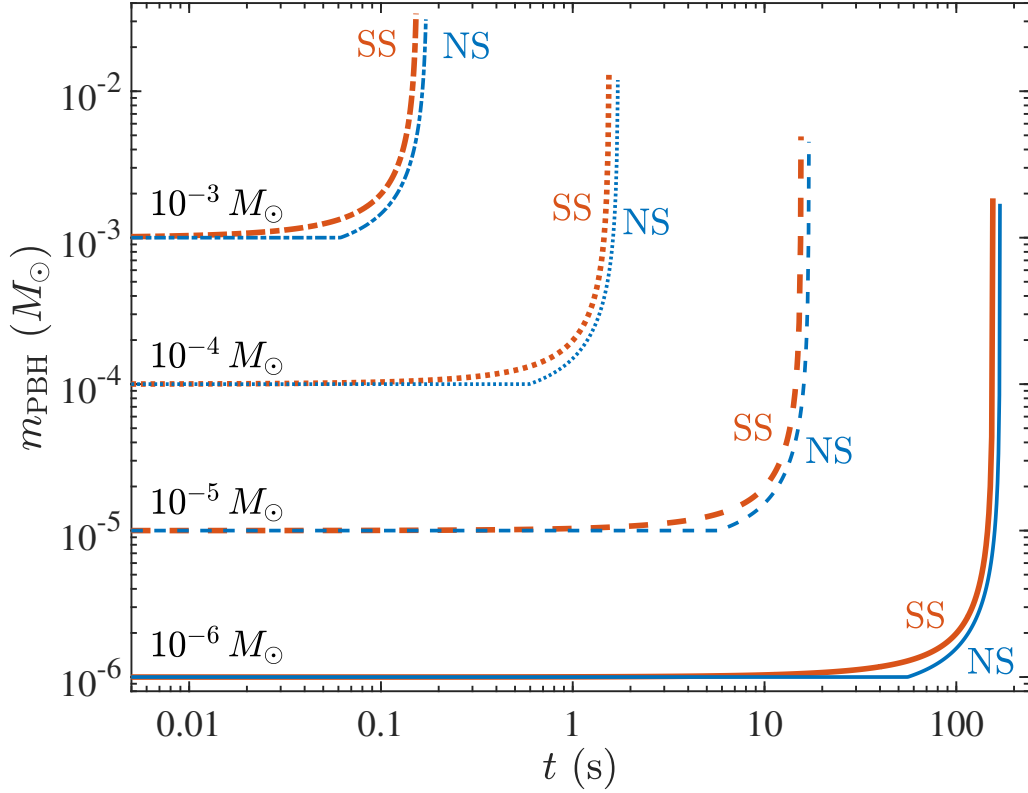


Figure 2. Evolution of the PBH mass. For the dash-dotted, dotted, dashed, and solid curves, the initial mass of the PBH is taken as 10^{-3} , 10^{-4} , 10^{-5} , and $10^{-6} M_{\odot}$, respectively. The mass of the compact star is $1.4 M_{\odot}$, which is assumed to be either an SS (thick curves) or an NS (thin curves).

et al. 2020; Aguayo-Ortiz et al. 2021). Such a value is appropriate for most of the density range in NSs and SSs (Potekhin et al. 2013; Xia et al. 2021).

2.4. Equation of Motion

During the inspiral, we assume that the compact star structure inside r keeps unchanged and the whole compact star remains spherically symmetric to its center. Thus the equation of motion can be written in the relative-motion frame as

$$\ddot{\mathbf{r}} = -\frac{MM_r\mathbf{r}}{M_{\text{CS}}r^3} + \frac{M\mathbf{F}_{\text{DF}}}{m_{\text{PBH}}M_{\text{CS}}} + \frac{\mathbf{F}_{\text{acc}}}{m_{\text{PBH}}} - \frac{32}{5} \frac{(M_r + m_{\text{PBH}})M_r m_{\text{PBH}}}{r^4} \left[1 + \frac{M_r + m_{\text{PBH}}}{r} \left(-\frac{743}{336} - \frac{11}{4} \frac{M_r m_{\text{PBH}}}{(M_r + m_{\text{PBH}})^2} \right) \right] \mathbf{v}, \quad (8)$$

where $M = M_{\text{CS}} + m_{\text{PBH}}$ is the total mass of the system. The last post-Newtonian term (Blanchet 2014) is introduced to account for the GW energy-loss.

The PBH is initially assumed to be located at the surface of the compact star, with a Keplerian velocity ($\sqrt{M/R_X}$, X stands for SS or NS) in a circular orbit. We terminate our calculation when $m_{\text{PBH}}/r = 1/12$, which means r reduces to a value comparable to the innermost stable circular orbit of the PBH and the post-Newtonian method loses its accuracy (Blanchet et al. 2011).

3. BINARY EVOLUTION

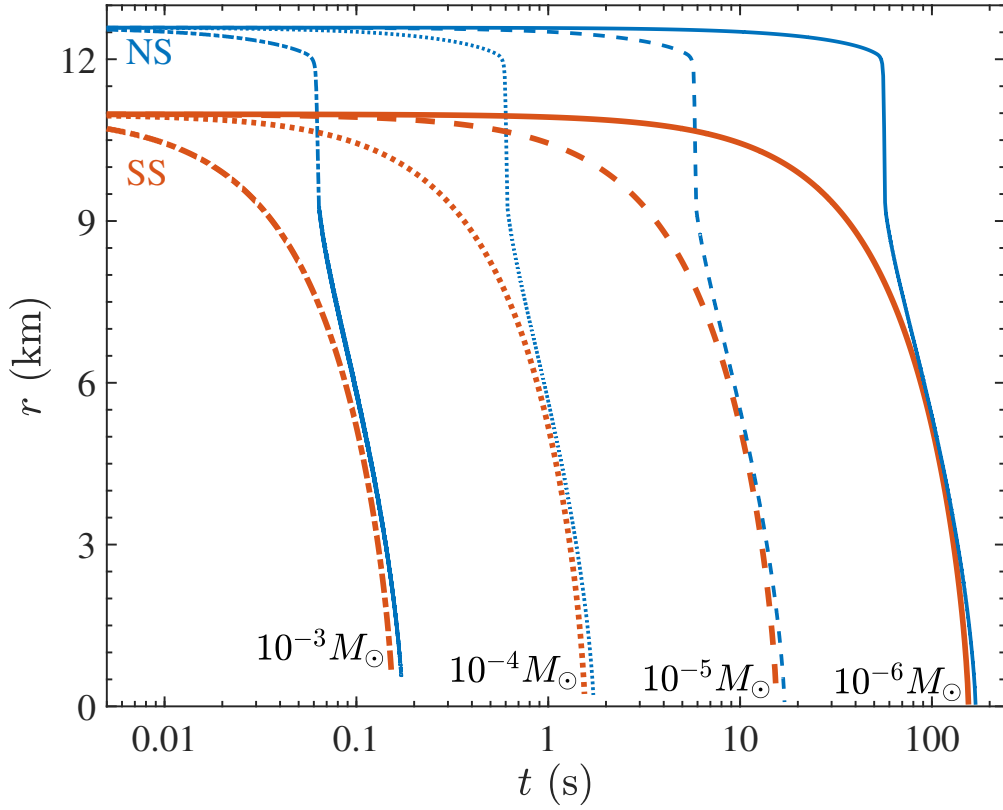


Figure 3. Evolution of the separation between the PBH and the compact star center. Line styles are the same as in Figure 2.

We have solved Equation 8 numerically. For the initial mass of the PBH, we take four typical values, i.e., 10^{-3} , 10^{-4} , 10^{-5} , and $10^{-6} M_{\odot}$. As for the compact star, we assume that it is either an SS or an NS, both with an initial mass of $M_0 = 1.4 M_{\odot}$. Figure 2 shows the evolution of the PBH mass. As expected, a PBH with a larger initial mass accretes faster. Moreover, the mass of the PBH interacting with an SS increases faster than that of the corresponding NS case. This is due to the large surface density of the SS. Note that in all our calculations, the condition of $m_{\text{PBH}} \ll M_{\text{CS}}$ is satisfied so that Equation 6 is applicable.

Figure 3 shows the evolution of the separation between the PBH and the center of the compact star. We see that the PBHs quickly inspiral inward as its mass increases. At the end of our calculation, the PBH almost settles at the center of the compact star, which means the remnant matter of the compact star will soon be completely swallowed by the black hole (Blanchet et al. 2011). In the NS cases, the separation decreases sharply in the range of $9 \text{ km} \lesssim r \lesssim 12 \text{ km}$. This is because the sound speed and density of the NS increase quickly in the region. As a result, the Mach number drops to an intermediate value, leading to an enhancement in the dynamical friction (Kim & Kim 2007).

Figure 4 illustrates the evolution of the quantity $m_{\text{PBH}} r^2$. It is interesting to note that Génolini et al. (2020) suggested that $m_{\text{PBH}} r^2$ is an adiabatic invariant during the inspiral. Our Figure 4 shows that $m_{\text{PBH}} r^2$ is roughly constant only at the very early stage of the inspiral, while it generally decreases in the latter process. The later decreasing of $m_{\text{PBH}} r^2$ may be caused by two reasons. First, the constant- $m_{\text{PBH}} r^2$ approximation is only valid in the deep subsonic regime, but the PBH moves at a speed comparable or larger than the sound

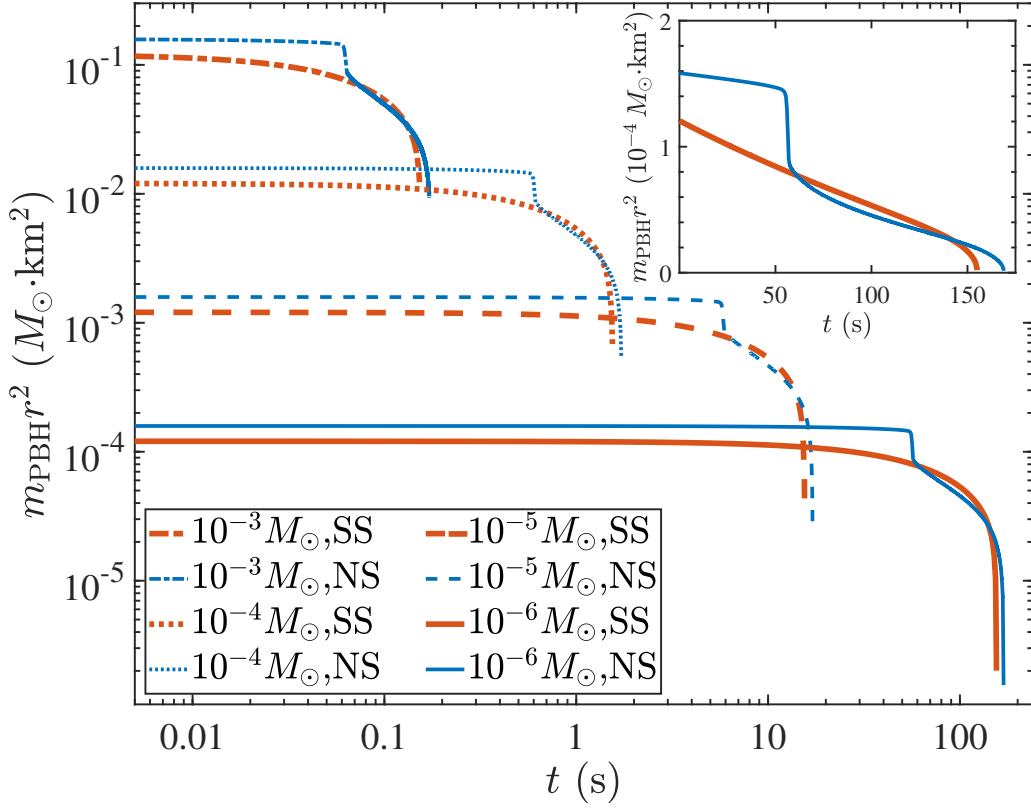


Figure 4. Evolution of $m_{\text{PBH}}r^2$. The inserted panel at the upper-right corner shows the $10^{-6} M_{\odot}$ PBH case on linear scale. Line styles are the same as in Figure 2.

speed. Second, when the PBH decelerates to a subsonic speed, it becomes very massive and it is also near the center of the compact star. As a result, the post-Newtonian term dominates the dynamical evolution.

4. GRAVITATIONAL WAVE SIGNAL

Under the quadrupole approximation, the leading-order GWs of a point mass moving inside a spherical object is similar to the case of two point masses (Nazin & Postnov 1995; Ginat et al. 2020). As a result, the GW waveforms of a PBH moving inside a compact star are (Creighton & Anderson 2011)

$$h_+ = -\frac{4\mu v^2}{D_L} \cos 2\varphi, \quad (9)$$

$$h_{\times} = -\frac{4\mu v^2}{D_L} \sin 2\varphi, \quad (10)$$

where $\mu = m_{\text{PBH}}M_{\text{CS}}/M$ is the reduced mass, D_L is the luminosity distance, φ is the orbital phase. Here the system is assumed to be face-on. Taking the distance as $D_L = 1$ kpc, the GW strain amplitude $h = 4\mu v^2/D_L$ is shown in Figure 5. Generally, the strain amplitude h decays with time. But it is interesting to note that there is obvious difference between the two curves corresponding to SS and NS. Thus the GW signal may be used to probe the EoS of dense matter.

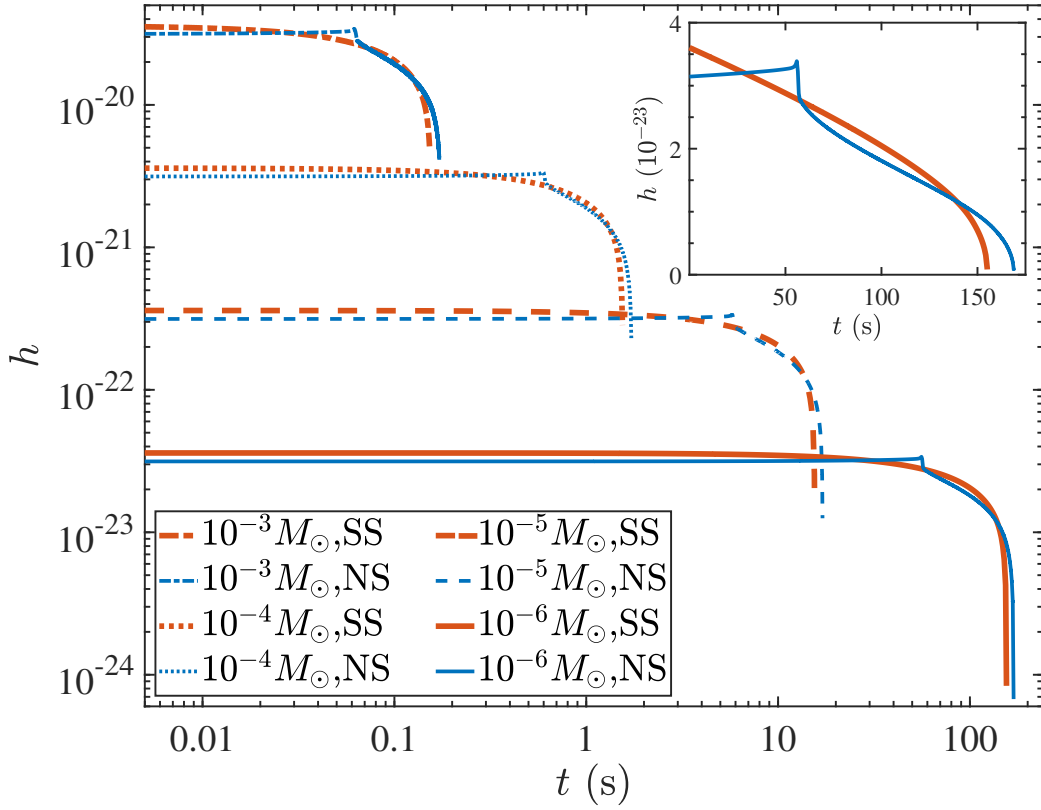


Figure 5. Evolution of the strain amplitude of the gravitational waves. The inserted panel at the upper-right corner shows the $10^{-6} M_{\odot}$ PBH case on linear scale. Line styles are the same as in Figure 2.

To decide whether the GW signal can be detected by a particular GW detector or not, it is useful to calculate the GW strain spectral amplitude (Moore et al. 2015; Zou et al. 2020)

$$h_f = 2f^{1/2} \left| \tilde{h}(f) \right|, \quad (11)$$

and compare it with the sensitivity of GW detectors. Here $\tilde{h}(f)$ is an average of the Fourier transforms of h_+ and h_{\times} at frequency f . Actually, h_f is the square root of the GW power spectral density. In Figure 6, we illustrate h_f in a frequency range of $\sqrt{M_0/R_X^3}/\pi \leq f \leq \sqrt{4\rho_c/(3\pi)}$, where ρ_c is the central density of the compact star. Beyond this main frequency range (3 – 5 kHz) of the GW signals, our calculation of $\tilde{h}(f)$ is significantly polluted by spectral leakage. Comparing h_f with the sensitivity curves of various GW detectors, we can see that the GWs from such a PBH system containing a $10^{-4} M_{\odot}$ black hole at 1 kpc away can be detected by the current Advanced LIGO and Advanced Virgo, while the upcoming LIGO A+ upgrade² and the next generation detectors such as Einstein Telescope³ and Cosmic Explorer⁴ can even detect the GWs from an inspiraling $10^{-5} M_{\odot}$ PBH. For a Jovian-mass PBH, due to the strong GW emission power, the detection horizon can even be pushed to megaparsecs by the next generation detectors.

² <https://dcc-lho.ligo.org/LIGO-T2000012/public>

³ <http://www.et-gw.eu/index.php/etsensitivities>

⁴ <https://cosmicexplorer.org/researchers.html>

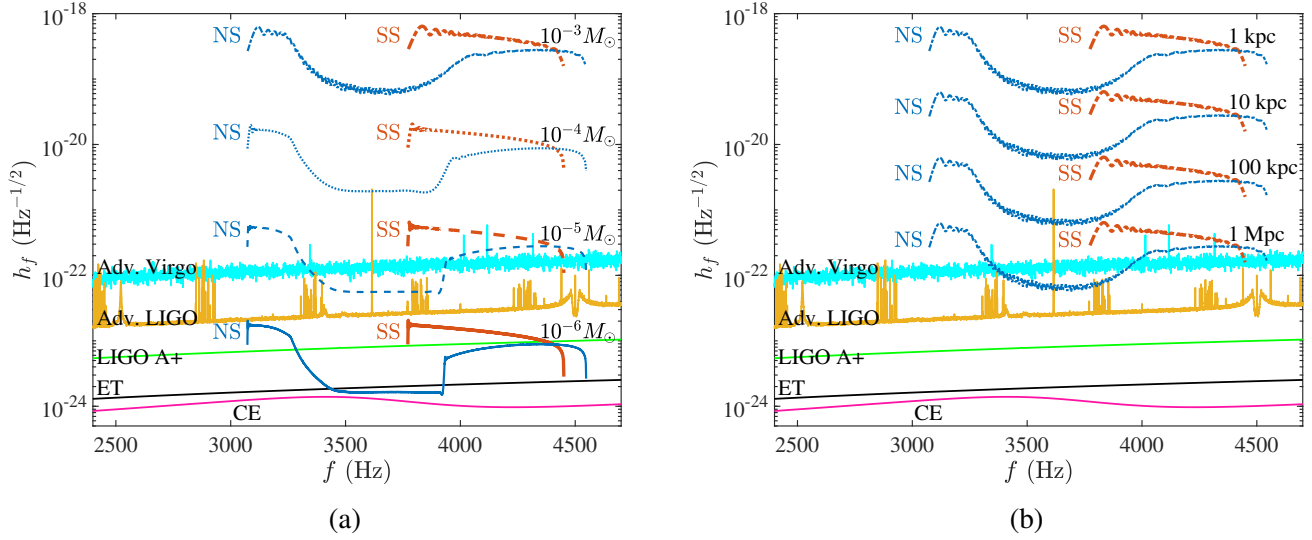


Figure 6. Strain spectral amplitude of GWs against frequency for a PBH inspiraling inside a compact star. In Panel (a), the system is fixed at 1 kpc away, but different initial masses are assumed for the PBH and are marked near the corresponding curves. In Panel (b), the initial mass of the PBH is fixed as $10^{-3} M_\odot$, but the systems are put at different D_L (see the marked values). Sensitivity curves of Advanced Virgo, Advanced LIGO, LIGO A+ upgrade, Einstein Telescope (ET), and Cosmic Explorer (CE) are plotted for a direct comparison. Other line styles are the same as in Figure 2.

Figure 6 clearly shows that although GWs in the NS case and the SS case have similar amplitudes, the shape of the detailed h_f curves actually is quite different for these two EoSs. For example, h_f in the SS cases generally decreases homogeneously with the increase of the frequency, while h_f in the NS cases shows a concavity at intermediate frequencies. As a result, GW detectors working in kilohertz can hopefully help us probe the EoS of dense matter through signals from PBHs inspiraling inside compact stars.

5. SUMMARY AND DISCUSSION

The process of a planetary-mass PBH inspiraling inside a compact star is investigated in detail. Such a process is of great interest for constraining PBH's composition fraction of dark matter. The effects of dynamical friction, accretion, and GW emission on the motion of the PBH are taken into account. Two kinds of compact stars are considered, i.e., SSs and normal NSs. It is found that the resulting GW signals show significant difference between the two cases. Encouragingly, GW emission from an inspiraling $10^{-4} M_\odot$ PBH at a distance of 1 kpc away from us can be detected by the current Advanced LIGO and Advanced Virgo detectors. Moreover, future GW detectors such as the Einstein Telescope and Cosmic Explorer can not only detect a $10^{-5} M_\odot$ PBH case at 1 kpc but also push the detection horizon of a Jovian-mass PBH case to megaparsecs. Note that the GW frequencies are near the high end of the sensitivity curve for most ground-based interferometers. Future ad hoc detectors working at kilohertz frequency like Neutron Star Extreme Matter Observatory (Ackley et al. 2020) will be powerful tools for probing the EoSs of dense matter.

Our dynamical equation (Equation 8) is invalid at the final stage when the whole compact star is to be swallowed by the PBH to form a stellar mass black hole. In our study, we did not calculate the GWs emitted at this final stage. However, since the PBH has moved to the central region of the compact star at the end

of our calculation, the accretion by the black hole should be highly spherical and the GWs are expected to be much weaker according to Birkhoff’s theorem. In our modeling, we have omitted the spinning of the compact star for simplicity. But note that the rotation of the compact star would not affect the results significantly, because even a millisecond pulsar rotates much slower than its Keplerian velocity (Génolini et al. 2020). Another approximation is that a constant λ is adopted during our calculations. To overcome this weakness, the GW signals should be calculated through full general relativistic hydrodynamic simulations, which is beyond the scope of the current study.

Before the PBH contacts the NS/SS surface and begins its journey inside the compact star, it orbits around its host as a very close-in object, which will also emit strong GWs. Such GWs may be recognized as originating from a “planet”-compact star system. Geng et al. (2015) and Kuerban et al. (2020) have suggested that GWs from such “planet”-compact star systems could be efficiently used to identify strange quark planets, because a normal matter planet will be tidally disrupted by the compact star when it is still further away so that no GWs are available (Geng et al. 2015; Kuerban et al. 2020). Here, we would like to further remind that the possibility that the “planet” is actually a PBH should be further repelled before finally identifying it as a strange quark planet. The GWs emitted by the PBH inspiraling inside its host compact star, as calculated by us in this study, can help us on this task. The merging of a strange quark planet with an SS will only produce some kind of ringing-down in GWs, while a PBH will tunnel through its host and produce complicated GW patterns as demonstrated in this study.

PBHs colliding with compact stars are also hypothetically associated with many other interesting phenomena, including the formation of solar mass black holes (Takhistov et al. 2021) and fast radio bursts (Abramowicz et al. 2018; Kainulainen et al. 2021). Future observations of the GWs will help constrain these hypotheses.

This work is supported by the National Natural Science Foundation of China (Grant Nos. 11873030, 12041306, U1938201), by National SKA Program of China No. 2020SKA0120300, by the National Key R&D Program of China (2021YFA0718500), and by the science research grants from the China Manned Space Project with NO. CMS-CSST-2021-B11.

REFERENCES

- Abbott, B. P., Abbott, R., Abbott, T. D., et al. 2018, *PhRvL*, 121, 161101, doi: [10.1103/PhysRevLett.121.161101](https://doi.org/10.1103/PhysRevLett.121.161101)
- . 2019, *Physical Review X*, 9, 011001, doi: [10.1103/PhysRevX.9.011001](https://doi.org/10.1103/PhysRevX.9.011001)
- Abramowicz, M. A., Bejger, M., & Wielgus, M. 2018, *ApJ*, 868, 17, doi: [10.3847/1538-4357/aae64a](https://doi.org/10.3847/1538-4357/aae64a)
- Ackley, K., Adya, V. B., Agrawal, P., et al. 2020, *PASA*, 37, e047, doi: [10.1017/pasa.2020.39](https://doi.org/10.1017/pasa.2020.39)
- Aguayo-Ortiz, A., Tejada, E., Sarbach, O., & López-Cámara, D. 2021, *MNRAS*, 504, 5039, doi: [10.1093/mnras/stab1127](https://doi.org/10.1093/mnras/stab1127)
- Alcock, C., Farhi, E., & Olinto, A. 1986, *ApJ*, 310, 261, doi: [10.1086/164679](https://doi.org/10.1086/164679)
- Annala, E., Gorda, T., Kurkela, A., & Vuorinen, A. 2018, *PhRvL*, 120, 172703, doi: [10.1103/PhysRevLett.120.172703](https://doi.org/10.1103/PhysRevLett.120.172703)
- Blanchet, L. 2014, *Living Reviews in Relativity*, 17, 2, doi: [10.12942/lrr-2014-2](https://doi.org/10.12942/lrr-2014-2)
- Blanchet, L., Spallicci, A., & Whiting, B. 2011, *Mass and Motion in General Relativity*, Vol. 162 (Springer, Dordrecht), doi: [10.1007/978-90-481-3015-3](https://doi.org/10.1007/978-90-481-3015-3)
- Bodmer, A. R. 1971, *PhRvD*, 4, 1601, doi: [10.1103/PhysRevD.4.1601](https://doi.org/10.1103/PhysRevD.4.1601)
- Bondi, H. 1952, *MNRAS*, 112, 195, doi: [10.1093/mnras/112.2.195](https://doi.org/10.1093/mnras/112.2.195)

- Cantó, J., Raga, A. C., Esquivel, A., & Sánchez-Salcedo, F. J. 2011, *MNRAS*, 418, 1238, doi: [10.1111/j.1365-2966.2011.19574.x](https://doi.org/10.1111/j.1365-2966.2011.19574.x)
- Capela, F., Pshirkov, M., & Tinyakov, P. 2013, *PhRvD*, 87, 123524, doi: [10.1103/PhysRevD.87.123524](https://doi.org/10.1103/PhysRevD.87.123524)
- Carr, B., & Kühnel, F. 2020, *Annual Review of Nuclear and Particle Science*, 70, 355, doi: [10.1146/annurev-nucl-050520-125911](https://doi.org/10.1146/annurev-nucl-050520-125911)
- Creighton, J., & Anderson, W. 2011, *Gravitational-Wave Physics and Astronomy: An Introduction to Theory, Experiment and Data Analysis*. (Wiley-VCH), doi: [10.1002/9783527636037](https://doi.org/10.1002/9783527636037)
- East, W. E., & Lehner, L. 2019, *PhRvD*, 100, 124026, doi: [10.1103/PhysRevD.100.124026](https://doi.org/10.1103/PhysRevD.100.124026)
- Edgar, R. 2004, *NewAR*, 48, 843, doi: [10.1016/j.newar.2004.06.001](https://doi.org/10.1016/j.newar.2004.06.001)
- Farhi, E., & Jaffe, R. L. 1984, *PhRvD*, 30, 2379, doi: [10.1103/PhysRevD.30.2379](https://doi.org/10.1103/PhysRevD.30.2379)
- Geng, J., Li, B., & Huang, Y. 2021, *The Innovation*, 2, 100152, doi: [10.1016/j.xinn.2021.100152](https://doi.org/10.1016/j.xinn.2021.100152)
- Geng, J. J., Huang, Y. F., & Lu, T. 2015, *ApJ*, 804, 21, doi: [10.1088/0004-637X/804/1/21](https://doi.org/10.1088/0004-637X/804/1/21)
- Génolini, Y., Serpico, P. D., & Tinyakov, P. 2020, *PhRvD*, 102, 083004, doi: [10.1103/PhysRevD.102.083004](https://doi.org/10.1103/PhysRevD.102.083004)
- Ginat, Y. B., Glanz, H., Perets, H. B., Grishin, E., & Desjacques, V. 2020, *MNRAS*, 493, 4861, doi: [10.1093/mnras/staa465](https://doi.org/10.1093/mnras/staa465)
- Guerra Chaves, A., & Hinderer, T. 2019, *Journal of Physics G Nuclear Physics*, 46, 123002, doi: [10.1088/1361-6471/ab45be](https://doi.org/10.1088/1361-6471/ab45be)
- Horowitz, C. J., & Reddy, S. 2019, *PhRvL*, 122, 071102, doi: [10.1103/PhysRevLett.122.071102](https://doi.org/10.1103/PhysRevLett.122.071102)
- Huang, Y. F., & Yu, Y. B. 2017, *ApJ*, 848, 115, doi: [10.3847/1538-4357/aa8b63](https://doi.org/10.3847/1538-4357/aa8b63)
- Itoh, N. 1970, *Progress of Theoretical Physics*, 44, 291, doi: [10.1143/PTP.44.291](https://doi.org/10.1143/PTP.44.291)
- Kainulainen, K., Nurmi, S., Schiappacasse, E. D., & Yanagida, T. T. 2021, *PhRvD*, 104, 123033, doi: [10.1103/PhysRevD.104.123033](https://doi.org/10.1103/PhysRevD.104.123033)
- Khlopov, M. Y. 2010, *Research in Astronomy and Astrophysics*, 10, 495, doi: [10.1088/1674-4527/10/6/001](https://doi.org/10.1088/1674-4527/10/6/001)
- Kim, H., & Kim, W.-T. 2007, *ApJ*, 665, 432, doi: [10.1086/519302](https://doi.org/10.1086/519302)
- Kuerban, A., Geng, J.-J., & Huang, Y.-F. 2019, in *American Institute of Physics Conference Series*, Vol. 2127, Xiamen-CUSTIPEN Workshop on the Equation of State of Dense Neutron-Rich Matter in the Era of Gravitational Wave Astronomy, 020027, doi: [10.1063/1.5117817](https://doi.org/10.1063/1.5117817)
- Kuerban, A., Geng, J.-J., Huang, Y.-F., Zong, H.-S., & Gong, H. 2020, *ApJ*, 890, 41, doi: [10.3847/1538-4357/ab698b](https://doi.org/10.3847/1538-4357/ab698b)
- Kurita, Y., & Nakano, H. 2016, *PhRvD*, 93, 023508, doi: [10.1103/PhysRevD.93.023508](https://doi.org/10.1103/PhysRevD.93.023508)
- Lai, X., Zhou, E., & Xu, R. 2019, *European Physical Journal A*, 55, 60, doi: [10.1140/epja/i2019-12720-8](https://doi.org/10.1140/epja/i2019-12720-8)
- Mondal, C., & Gulminelli, F. 2021, arXiv e-prints, arXiv:2111.04520. <https://arxiv.org/abs/2111.04520>
- Moore, C. J., Cole, R. H., & Berry, C. P. L. 2015, *Classical and Quantum Gravity*, 32, 015014, doi: [10.1088/0264-9381/32/1/015014](https://doi.org/10.1088/0264-9381/32/1/015014)
- Nazin, S. N., & Postnov, K. A. 1995, *A&A*, 303, 789
- Ogilvie, G. I. 2014, *ARA&A*, 52, 171, doi: [10.1146/annurev-astro-081913-035941](https://doi.org/10.1146/annurev-astro-081913-035941)
- Oppenheimer, J. R., & Volkoff, G. M. 1939, *Physical Review*, 55, 374, doi: [10.1103/PhysRev.55.374](https://doi.org/10.1103/PhysRev.55.374)
- Ostriker, E. C. 1999, *ApJ*, 513, 252, doi: [10.1086/306858](https://doi.org/10.1086/306858)
- Pani, P., & Loeb, A. 2014, *JCAP*, 2014, 026, doi: [10.1088/1475-7516/2014/06/026](https://doi.org/10.1088/1475-7516/2014/06/026)
- Pearson, J. M., Chamel, N., Potekhin, A. Y., et al. 2018, *MNRAS*, 481, 2994, doi: [10.1093/mnras/sty2413](https://doi.org/10.1093/mnras/sty2413)
- Potekhin, A. Y., Fantina, A. F., Chamel, N., Pearson, J. M., & Goriely, S. 2013, *A&A*, 560, A48, doi: [10.1051/0004-6361/201321697](https://doi.org/10.1051/0004-6361/201321697)
- Richards, C. B., Baumgarte, T. W., & Shapiro, S. L. 2021, *PhRvD*, 103, 104009, doi: [10.1103/PhysRevD.103.104009](https://doi.org/10.1103/PhysRevD.103.104009)
- Shibata, M., Zhou, E., Kiuchi, K., & Fujibayashi, S. 2019, *PhRvD*, 100, 023015, doi: [10.1103/PhysRevD.100.023015](https://doi.org/10.1103/PhysRevD.100.023015)
- Shima, E., Matsuda, T., Takeda, H., & Sawada, K. 1985, *MNRAS*, 217, 367, doi: [10.1093/mnras/217.2.367](https://doi.org/10.1093/mnras/217.2.367)
- Takhistov, V., Fuller, G. M., & Kusenko, A. 2021, *PhRvL*, 126, 071101, doi: [10.1103/PhysRevLett.126.071101](https://doi.org/10.1103/PhysRevLett.126.071101)
- Tolman, R. C. 1939, *Physical Review*, 55, 364, doi: [10.1103/PhysRev.55.364](https://doi.org/10.1103/PhysRev.55.364)
- Wang, X., Huang, Y.-F., & Li, B. 2021, arXiv e-prints, arXiv:2109.15161. <https://arxiv.org/abs/2109.15161>

- Wang, X., Kuerban, A., Geng, J.-J., et al. 2021, PhRvD, 104, 123028, doi: [10.1103/PhysRevD.104.123028](https://doi.org/10.1103/PhysRevD.104.123028)
- Witten, E. 1984, PhRvD, 30, 272, doi: [10.1103/PhysRevD.30.272](https://doi.org/10.1103/PhysRevD.30.272)
- Xia, C., Zhu, Z., Zhou, X., & Li, A. 2021, Chinese Physics C, 45, 055104, doi: [10.1088/1674-1137/abea0d](https://doi.org/10.1088/1674-1137/abea0d)
- Zel'dovich, Y. B., & Novikov, I. D. 1967, Soviet Ast., 10, 602
- Zou, Z.-C., Zhou, X.-L., & Huang, Y.-F. 2020, Research in Astronomy and Astrophysics, 20, 137, doi: [10.1088/1674-4527/20/9/137](https://doi.org/10.1088/1674-4527/20/9/137)